Oxygen-induced magnetic surface states on the (0001) surfaces of heavy lanthanide metals

C. Schüßler-Langeheine,[1] H. Ott,[1] A. Yu. Grigoriev,[1,2] A. Möller,[1] R. Meier,[1] Z. Hu,[1] Chandan Mazumdar,[1] G. Kaindl,[1] and E. Weschke[1]

[1]*Institut für Experimentalphysik, Freie Universität Berlin, Arnimallee 14, D-14195 Berlin, Germany*

[2] *Institute of Physics, St. Petersburg State University, Uljanovskaja 1, 198904 St. Petersburg, Russia*

(Received 16 January 2001; revised manuscript received 23 May 2001; published 20 May 2002)

Oxygen adsorption on the close-packed surfaces of trivalent heavy lanthanide metals leads to the formation of well-ordered surface-oxide systems. These systems are characterized by fully occupied oxygen-induced surface states, resembling the surface states of the clean metal surfaces. For the magnetic lanthanides, these states exhibit temperature-dependent magnetic splittings with constant finite values above the respective highest magnetic ordering temperatures, T^*. Angle-resolved photoemission from Gd to Ho reveals a systematic behavior of the splittings: the magnitudes are proportional to the $4f$-spin moment and their temperature dependencies scale with T^*.

DOI: 10.1103/PhysRevB.65.214410 PACS number(s): 75.70.Ak, 75.70.Rf, 79.60.−i, 73.20.At

I. INTRODUCTION

The magnetic properties of the lanthanide metals are strongly determined by the atomiclike $4f$ moments, which persist in the solid state.[1] Long-range magnetic order in these systems is induced by an indirect exchange interaction between the $4f$ moments via the polarization of conduction electrons, the so-called Ruderman-Kittel-Kasuya-Yosida (RKKY) interaction.[2] This interaction, in competition with anisotropies and magnetoelastic energies, leads to a variety of magnetic structures, including ferromagnetic, helical antiferromagnetic, and conical ferrimagnetic phases.[3–6] The RKKY coupling mechanism is particularly sensitive to details of the Fermi surface, and the relation of the magnetic structures to the so-called nesting features is well established, both theoretically[4] and experimentally.[7,8]

Less well understood and a topic of current research is the influence of magnetic ordering on the details of the temperature-dependent valence-electronic structure.[9–19] Theoretical calculations were performed particularly for ferromagnetic Gd metal. In a many-body treatment by Nolting *et al.*, the temperature dependencies of the magnetic exchange splitting and the spin polarization of valence states were found to vary across the Brillouin zone.[11] Considering two extreme cases, itinerant *s*-like states were found to be sensitive to long-range magnetic order, leading to an energy splitting that reflects the net magnetization and hence vanishes at the Curie temperature, T_C. Resembling the characteristics of the valence states within the Stoner model of band ferromagnetism,[20] this behavior is referred to as Stoner-like. In contrast, the splitting of more localized *d*-like states in the vicinity of the Fermi energy, E_F, depends only on the temperature independent local $4f$ moment and hence was found to be essentially temperature independent, persisting into the paramagnetic phase. In a disordered local-moment system, such as Gd metal at finite temperatures, the spin projection of a given valence state onto the magnetization direction is not well defined. This characteristic, often called spin mixing, leads to a decrease of the spin polarization with increasing temperature, vanishing in the paramagnetic phase.

The influence of the temperature-dependent magnetic order on the band structure of Gd was also studied by Sandratskii and Kübler using a model with a certain finite angle between the $4f$ moments in adjacent close-packed layers.[10,21] Here, the $4f$ magnetic structure forms a helix along the crystallographic *c* axis of hexagonal close-packed (hcp) Gd. This structure imposes a generalized translational symmetry, which allows a calculational treatment. In this model, the fully ordered ferromagnetic phase at zero Kelvin is reproduced by an infinite helix period; increasing temperature is simulated by a decreasing helix period. The results obtained within this model are similar to those of Nolting *et al.*, with energetically low-lying states displaying a Stoner-like behavior, while other states showing a more complex temperature-dependent redistribution of minority- and majority-spin contributions. Interestingly, the calculations revealed a magnetic splitting of valence states for certain regions of the Brillouin zone in this helical antiferromagnetic system despite the zero net magnetization, as long as the helix period is larger than ≈ 4 monolayers.[10] Such a helical antiferromagnetic structure exists, e.g., in Tb, Dy, and Ho, and exchange splittings were recently observed in their respective antiferromagnetic phases by angle-resolved photoemission (PE) for the Δ_2 states near the center of the Brillouin zone, Γ.[19] The exchange splitting of these states was found to be proportional to the $4f$-spin moment, indicating that the $4f$-$5d$ exchange integral does not change considerably across the lanthanide series.[19] Furthermore, these bulk-related valence states exhibit a Stoner-like temperature dependence of the magnetic splitting, essentially vanishing at the respective highest magnetic ordering temperature T^*,[9,19] in rather good agreement with the theoretical calculations for Gd metal.[11]

The search for pronounced spin-mixing behavior and temperature-independent magnetic splitting, on the other hand, raised some controversy. Resonances observed in the optical reflectivity of the lanthanide metals[22–25] were interpreted as a result of a temperature-independent energy splitting of states above and below E_F around the L high-symmetry point of the hcp Brillouin zone;[21] to our best knowledge, these states have not been directly observed by PE or inverse photoemission (IPE) up to now. Considering the calculations of Nolting *et al.* for bulk states in the vicin-

ity of E_F,[11] a good candidate for spin-mixing behavior is the localized, partially occupied surface state, present on all close-packed surfaces of the trivalent lanthanide metals.[26–29] And in fact, many studies concentrated on this *d*-like surface state.[12–18] Experimentally, however, it cannot be accessed by angle-resolved PE nor by IPE alone, since at low temperatures, the majority component is occupied, whereas the minority component is unoccupied. The close proximity to the Fermi energy aggravates the determination of the binding energy (BE) by either of the two methods and data suggesting Stoner-like[12,14,15] as well as spin-mixing behavior[13] were obtained.

Particularly useful in this case has been scanning-tunneling spectroscopy (STS), which is capable of probing both occupied and unoccupied states in the vicinity of the E_F in a single experiment. By this method, the surface state on Gd(0001) was shown to have a temperature-dependent splitting with a finite residual value that stays constant above T_C.[16,17] A more recent STS study of the corresponding surface state on Tb(0001) by Bode *et al.*[18] revealed a behavior different to that of Gd, with the energy splitting decreasing even at temperatures of at least 30 K above the Néel temperature ($T_N \approx 230$ K). This deviation from Gd was suggested to be due to short-range antiferromagnetic correlations resembling the temperature-dependent helical structure above T_N. However, the above-mentioned study of the Δ_2 bulk states showed that their magnetic splitting behaves fully systematically, with no anomaly in the antiferromagnetic phases.[19]

Thus, the picture of electronic states with pronounced spin-mixing behavior evolving from these experiments still remains unsatisfactory, calling for a systematic study across the lanthanide series. For such a study, we have chosen a characteristic oxygen-induced surface state rather than the surface state of the clean close-packed surfaces, because the former is fully occupied and hence readily accessible by angle-resolved PE only, as demonstrated for the cases of Lu(0001) (Ref. 30) and Gd(0001).[31] This oxygen-induced surface state is characteristic of the well-ordered (1×1) surface-oxide system that can be readily prepared on the close-packed surfaces of the heavy trivalent lanthanide metals.

The paper is arranged as follows: Following this introduction, the second section is concerned with experimental details of the preparation and characterization of the oxygen-induced surface states. The magnetic properties of the surface states are discussed in the third section.

II. PREPARATION AND CHARACTERIZATION OF THE OXYGEN-INDUCED SURFACE STATE

The experiments were performed on the close-packed surfaces of ≈100-Å-thick lanthanide-metal films epitaxially grown *in situ* in ultrahigh vacuum (UHV) on W(110). On this substrate, the films grow in close-packed planes with high crystalline quality and very clean surfaces.[29,32] Corresponding to the (0001) surface of the hexagonal close-packed crystal structure of the heavy lanthanide metals, sharp hexagonal low-energy electron-diffraction (LEED) patterns are observed from these films. Well-ordered surface oxides were prepared by dosing ≈1 L (10^{-6} Torr sec) of molecular oxygen at a partial pressure of 5×10^{-9} mbar and subsequently annealing. The annealing temperature was limited by the onset of oxygen desorption, occuring around 350 K in the case of Gd, but not below 700 K in the case of Lu. These surface oxides exhibited long-range crystalline order as inferred from sharp (1×1) LEED patterns observed in all cases. The oxygen dose turned out to be uncritical; even larger doses up to ≈2.5 L lead to identical results. This indicates a passivation of the system after an initial oxidation of the surface. Such a passivation behavior was also found in an early oxidation study of Gd(0001), where a (1×1) LEED pattern persisted after oxygen doses of 100 L and even after exposure to ambient atmosphere for one hour.[33]

Angle-resolved PE experiments were carried out at the Berliner Elektronenspeicherring für Synchrotronstrahlung (BESSY I) with a laboratory PE spectrometer. In the case of Gd, data were recorded at the TGM 3, TGM 5, and TGM 6 beamlines using a VSW ARIES hemispherical electron energy analyzer with an angular resolution of ≈2°. The total-system energy resolution varied between 80 meV and 130 meV (full width at half maximum). The experiments on the Tb, Dy, Ho, and Lu surfaces were performed with a Scienta SES 200 analyzer operated in angle-resolving mode using 40.8-eV photons from a high-flux He resonance lamp selected by a grating monochromator. The total-energy resolution was set to 50 meV, and the angular resolution was ≈2°.

The typical changes of the electronic structure upon oxygen adsorption on the close-packed surfaces of trivalent lanthanide metals are shown in Fig. 1 for the example of Tb(0001). The $4f$ PE final-state multiplet of Tb metal is characterized by a well-separated ^8S component with a comparably low BE of ≈2.3 eV. Therefore, changes of both the $4f$ and the valence-band structures in the vicinity of E_F can be observed in detail in a single PE spectrum. The spectrum of the clean Tb(0001) surface (bottom), recorded at 50 K, displays emission from the occupied part of the surface state, *S*, directly at E_F, the Δ_2 states, as well as the ^8S component of the $4f$ multiplet, consisting of a bulk (*b*) and a surface (*s*) contribution, separated by a surface core-level shift of (270 ±30) meV.[34] The surface state *S* with essentially $d_{3z^2-r^2}$ character[26,27] was already mentioned in the introduction as a general feature of the close-packed surfaces of trivalent lanthanide metals.[29] Because it's derived from the bulk *d* band, *S* represents a Tamm state.[35] At low temperatures, the Δ_2 states exhibit an energy splitting due to the exchange interaction with the $4f$ states, with the high-BE component hidden by the $4f$ emission.[19]

The characteristics of oxygen adsorption can be inferred from the ^8S component of the $4f$ spectra. Upon oxygen adsorption, the surface component *s* is successively suppressed, being replaced by a new feature s_2 shifted by (580 ±30) meV with respect to *s*. This comparably large chemical shift is characteristic of strong chemisorption rather than weak physisorption,[36] suggesting an interpretation in terms of a surface oxide.

A fit analysis of the data of Fig. 1 shows that the BE and

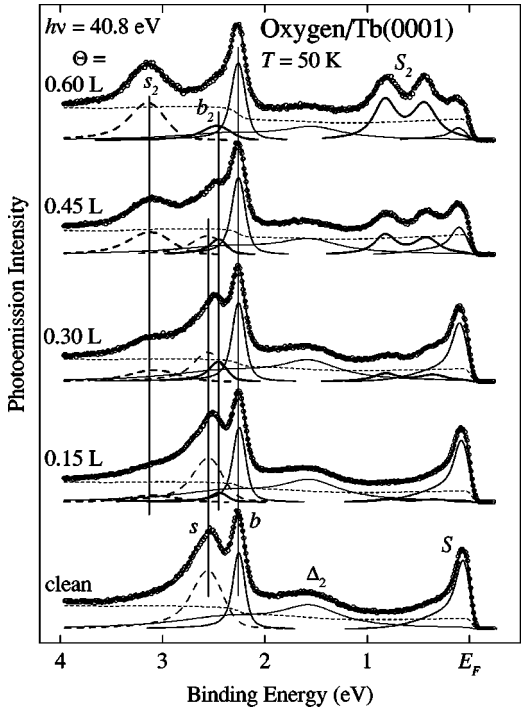

FIG. 1. Angle-resolved PE spectra recorded in normal-emission geometry from a clean Tb(0001) surface and at several stages of oxygen exposure. The spectra are normalized with respect to the total $4f$ intensity.

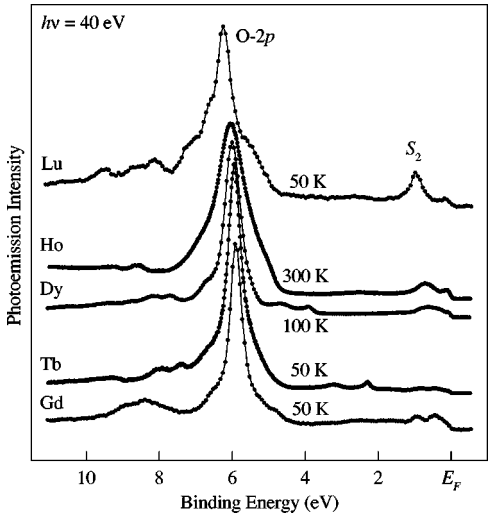

FIG. 2. Angle-resolved PE spectra recorded from the oxygen-covered (0001) surfaces of Gd, Tb, Dy, Ho, and Lu in normal-emission geometry at the given temperatures. Note that the spectrum of Ho was recorded at room temperature and hence exhibits substantial thermal broadening.

intensity of the bulk component *b*, normalized with respect to the total $4f$-spectral intensity, are essentially unchanged. The intensity of the $4f$ surface component *s* decreases, balanced by a new component s_2. The same behavior has been observed in the cases of Gd (Ref. 31) and Lu,[30] as well as Yb at low temperatures,[30] showing that oxygen adsorption on the close-packed surfaces of the heavy lanthanide metals under the present conditions takes place at the surface only with no diffusion into the bulk. As in the latter cases, a further oxygen-induced component b_2 is introduced for the fit analysis of the $4f$ spectra. In the case of Lu, this component is well resolved and can be readily interpreted in terms of $4f$ emission from the second layer being affected by the adsorption of oxygen in the surface layer.[30] For Gd, this component is also observed as a shoulder on the bulk $4f$ component, however, it is not as well resolved as for Lu.

In the PE spectra of Fig. 1, the concomitant changes in the valence-electronic structure are also readily observed. Upon oxygen adsorption, the intensity of the Δ_2 bulk states decreases. Such behavior of bulk bands during the surface adsorption of oxygen has been observed for other metals.[37] The most striking and important changes in the present context occur in the vicinity of E_F. The surface state *S* is suppressed, while a new feature S_2 occurs, which is split into two components at low temperatures. At an oxygen dose of ≈ 0.6 L, i.e., when the $4f$ component *s* is replaced by s_2, *S* is essentially replaced by S_2. As discussed further below, the oxygen-induced state S_2 displays the characteristics of a surface state. As in the case of the LEED patterns, higher doses of oxygen up to ≈ 2.5 L do not further affect the electronic structure, indicating a passivation of the surface after the first layer has been oxidized. Due to this passivation, oxygen deposition is uncritical and, once prepared, the films stay unchanged for more than one day under UHV conditions. Analogous results were obtained for the surfaces of the other trivalent lanthanide metals of this study.[31]

Oxygen adsorption under the present conditions does not lead to the formation of the trivalent lanthanide sesquioxides Ln_2O_3; these latter compounds are characterized by a much broader $4f$ emission and vanishing spectral intensity at E_F.[30,31] The distinctly different character of the present surface oxide is further corroborated by the characteristic O-$2p$ emission shown in Fig. 2. This figure displays PE spectra recorded from the oxygen-covered (0001) surfaces of Gd to Lu, giving an overview of the valence-electronic structure. The most intense feature in all spectra is the sharp O-$2p$ emission around 6-eV BE, which is the signature of dissociatively chemisorbed oxygen,[36,38] and which is distinctly different from the broad multicomponent O-$2p$ emission observed for Ln_2O_3.[30,31] In fact, the preparation of the sesquioxide on the close-packed surface of Gd was found to require heavy oxygen exposure of 300 L at 500 °C,[33] which was not applied here. Although a determination of the stoichiometry at the surface is not straightforward and has not been obtained here, an interpretation of the data in terms of monoxides is not unreasonable. While monoxides are not stable as bulk compounds, they could exist on the surface,[30] since a reduced valence at the surface is favored in many lanthanide systems due to the smaller number of nearest neighbors.[40] With the assumption of a reduced valence at the surface, it is resonable to draw an analogy between the present surface-oxide phase and the lanthanide monosulphides.[30] These latter systems are known as stable bulk compounds that exhibit metallic character and magnetic order.[39] In this context, it is to be noted that the bulk $4f$ BE of YbS is close to that of the

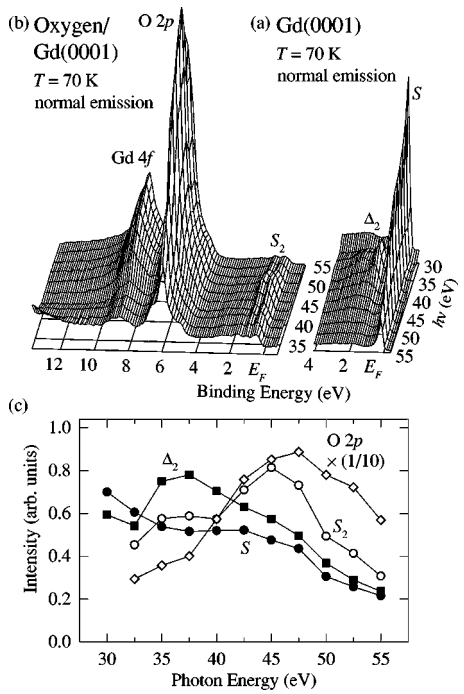

FIG. 3. Angle-resolved PE spectra of the Gd(0001) surface recorded in normal-emission geometry for various photon energies: (a) clean surface; (b) after oxygen adsorption. The spectra are normalized to the incident photon flux. Note the different photon energy axes in (a) and (b). (c) Corresponding integrated intensities of the oxygen-induced state (S_2, open circles) and the O-2p emission (open diamonds) in comparison to those of the surface state (S, solid circles) and of the Δ_2 band (solid squares) of clean Gd(0001).

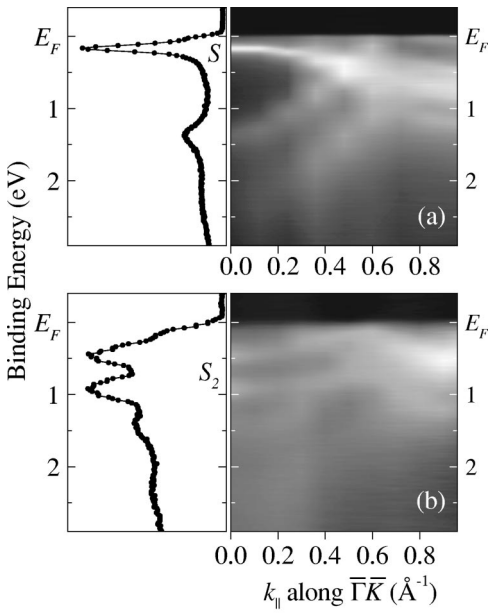

FIG. 4. Intensity plot of angle-resolved PE spectra recorded from (a) the clean and (b) the oxygen-covered Gd(0001) surfaces at various emission angles along $\overline{\Gamma K}$. ($\overline{K}$ corresponds to $k_\parallel = 1.15$ Å^{-1}). Data were obtained at (a) 26 K and (b) 70 K, i.e., well below the Curie temperature. Respective PE spectra at $\overline{\Gamma}$ ($k_\parallel = 0$) are shown on the left.

respective surface-oxide component on close-packed Yb(111), supporting an interpretation in terms of a similar chemical environment.[30,41]

Figure 2 demonstrates that the changes of the surface-electronic structure upon oxygen adsorption are very similar for all the lanthanides of the present study. All spectra exhibit the sharp O-2p emission characteristic of the surface-oxide phase. The figure also shows that the oxygen-induced surface state S_2 is present in all cases. It consists of a single component for nonmagnetic Lu, while a splitting can be clearly seen for Gd and Tb. For Dy and Ho, the splitting is too small to be resolved in this overview spectrum.

Before turning to the discussion of the electronic structure in connection with magnetic order, S_2 is characterized in more detail in order to show that it closely resembles the surface state S of the clean surfaces, however, it is fully occupied. Figure 3 displays sets of angle-resolved PE spectra recorded (i) from the clean Gd(0001) surface and (ii) after oxygen adsorption. They were taken in normal-emission geometry at various photon energies and hence probe different points in momentum space along the ΓA high-symmetry direction of the hcp Brillouin zone. The spectra of the clean surface are dominated by emission from the surface state, with decreasing intensity upon increasing photon energy. As characteristic for an electron state of two-dimensional character, no variation of the BE is observed for S. The spectra of Fig. 3(b) were recorded over a larger BE range, including the oxygen-induced state S_2 as well as the Gd-4f and O-2p emissions. Also in these spectra, none of the features changes its BE upon variation of the photon energy. This is expected in the case of the atomiclike 4f states. For the O-2p emission and S_2, the lack of dispersion supports the interpretation in terms of a two-dimensional character of the surface oxide as may be anticipated from the reaction of oxygen taking place at the surface only. In this respect, S_2 resembles the behavior of S.

Further information about the character of S_2 can be obtained from the relative PE cross sections of S_2 and O-2p, extracted from the integrated peak intensities in Fig. 3(b), in comparison to those of the surface state S and the Δ_2 band obtained from Fig. 3(a), as plotted in Fig. 3(c). The cross section of S (solid circles) decreases with increasing photon energy, exhibiting a weak maximum around 45 eV.[42] This overall decrease is also observed for the Δ_2 band (solid squares). The behavior of S_2 (open circles), on the other hand, is characterized by a pronounced maximum around 45 eV, rather following the cross-section behavior of the O-2p emission (open diamonds). This similarity of the PE cross sections indicates a significant mixing of O-2p and Gd-5d states at the surface upon the formation of S_2.

In addition to the two-dimensional character of S_2, the analogy to S is further established by the energy position and dispersion within the close-packed planes as shown in Figs. 4 and 5. Angle-resolved PE spectra of the valence-band region were recorded from Gd(0001) for various electron emission angles at temperatures well below the Curie temperature. The resulting PE intensities as a function of the BE and the in-plane component of the electron wave vector, $k_\parallel$, are

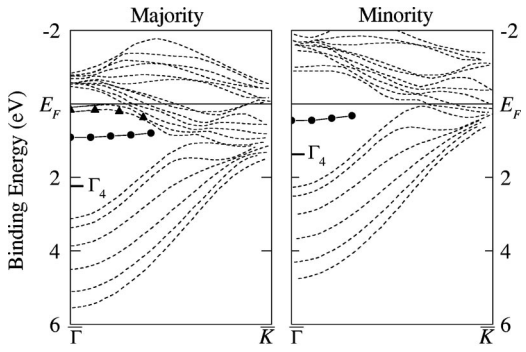

FIG. 5. Dispersions of the occupied part of the surface state *S* (triangles) and of the oxygen-induced surface state S_2 (circles). The dashed lines represent the layer-resolved band structure from a spin-resolved slab calculation for ferromagnetic Gd (from Ref. 26). The Γ_4 bars mark the experimentally determined critical-point energies of the Δ_2 band.

shown as gray-scale plots in Fig. 4, providing a direct image of the dispersion along the $\bar{\Gamma}\bar{K}$ high-symmetry direction of the surface Brillouin zone. On the left, corresponding normal-emission spectra are shown.

The behavior of the occupied part of *S* can be inferred from the data of the clean surface [Fig. 4(a)]. *S* exhibits a weak decrease of the BE towards the border of the surface Brillouin zone. The dispersion of *S* determined from the PE spectra is plotted in Fig. 5 (triangles), superimposed on a calculated, layer- and spin-resolved band structure of Gd(0001) (dashed lines, from Ref. 26). The comparison with these calculations shows that *S* is split off the *d* band that forms the *upper* edge of the band gap around $\bar{\Gamma}$ and hence can be identified as a Tamm-like surface state. The dispersion of *S* is flat in the vicinity of $\bar{\Gamma}$; towards $\bar{K}$, it decreases in energy, following the behavior of the *d* band.

The characteristics of the oxygen-induced surface state S_2 can be inferred from Fig. 4(b). Like *S*, it is located in the energy gap of the projected bulk band structure, but at higher BE's well below E_F, closer to the Δ_2 band, which forms the *lower* edge of the band gap. It is to be noted that the oxygen-induced band is in fact even closer to the Δ_2 band than suggested by the calculation, since the experimentally determined critical-point energy of Γ_4 is substantially closer to E_F, as indicated by the solid bars.[9] Like the surface state *S*, the oxygen-induced state S_2 (circles) shows a rather flat dispersion in the vicinity of $\bar{\Gamma}$. Along $\bar{\Gamma}\bar{K}$, it moves towards E_F, thus following the dispersion of the Δ_2 band. This is again the typical behavior of a Tamm surface state, split off the corresponding bulk band.[35]

Plotting the dispersion of the two components of S_2 in Fig. 5 separately in the spin-resolved band structures suggests that they represent majority and minority components of the oxygen-induced surface state. While such an interpretation is reasonable in view of the behavior of the surface state of clean Gd(0001), at least at low temperatures,[43] no information about the spin character was obtained from the present experiments. However, the energy splitting is clearly of magnetic origin, as discussed in more detail in the following section.

III. MAGNETIC PROPERTIES OF THE OXYGEN-INDUCED SURFACE STATE

The surface oxides on the close-packed surfaces of the lanthanide metals are characterized by an electronic structure, which is different from that of the nonmetallic trivalent sesquioxides. They rather show metallic character with substantial spectral weight at E_F and in this respect resemble the monosulfides. Since these latter compounds exhibit magnetic order, it is not unexpected that such a phenomenon occurs also in the present surface oxides, particularly since the surface layer is coupled to a magnetically ordered bulk. And in fact, a magnetic splitting of the oxygen-induced surface state S_2 is observed, exhibiting systematic behavior across the lan-

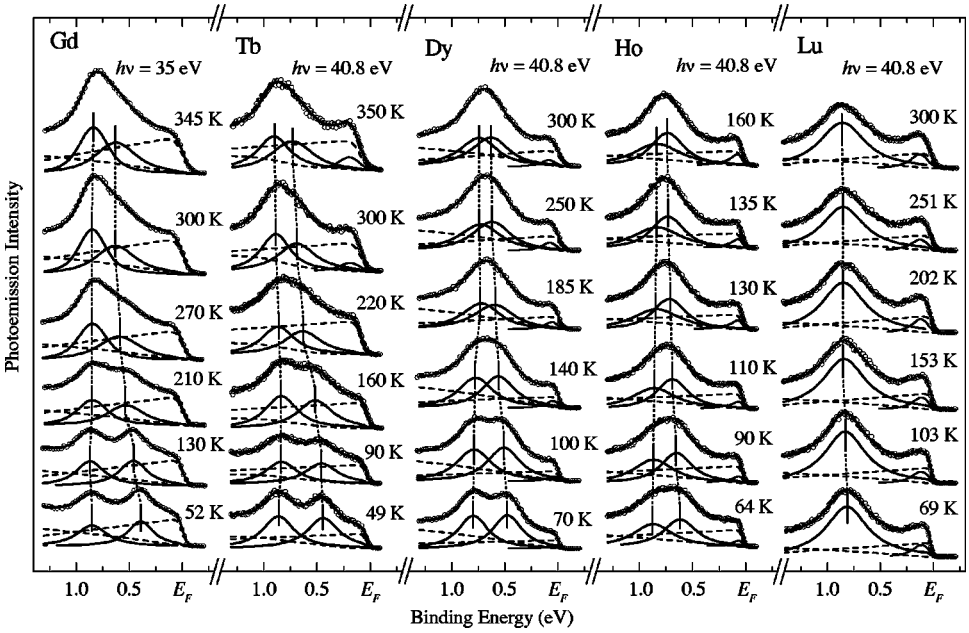

FIG. 6. Angle-resolved PE spectra of the oxygen-covered (0001) surfaces of Gd, Tb, Dy, Ho, and Lu at various temperatures together with the results of consistent least-squares-fit analyses.

thanide series, both as a function of temperature and the $4f$-spin moment. This is qualitatively evident from the compilation of angle-resolved PE spectra in Fig. 6, recorded in normal-emission geometry from the oxygen-covered close-packed surfaces of Gd to Ho and Lu.

For a detailed quantitative analysis of the spectra in Fig. 6, it is useful to consider first the nonmagnetic reference system Lu and to determine the pure thermal effects on the line shape. Lu is well suited, because its valence configuration is the same as that of the magnetic heavy lanthanides. The $4f$ shell of Lu is completely filled and hence carries no magnetic moment. In this particularly simple case, a least-squares-fit analysis can be readily applied to obtain a description of the temperature-dependent spectra (solid lines through the data points). It turns out that S_2 is described by a single symmetric Lorentzian line at all temperatures. The spectral shape does not change with temperature except for thermal broadening, described by a Gaussian convolution, and a slight shift of the BE from (790 ± 20) meV at 69 K to (840 ± 20) meV at 300 K. For a perfect description of the data, a weak contribution from remainders of the surface state near E_F was introduced. Furthermore, the background intensity due to emissions from other parts of the Brillouin zone and inelastic effects were taken into account (dashed lines). While in the case of Lu, S_2 is symmetric throughout the whole temperature series, this is not the case for the magnetic systems. For Gd to Ho, the oxygen-induced states exhibit an energy splitting at low temperatures, which decreases upon heating. The splitting is well resolved in the low-temperature spectra of Gd, Tb, and Dy, and it is still discernible as a shoulder in the case of Ho. The splitting decreases with increasing temperature up to the highest magnetic ordering temperature T^*; above T^*, the spectral shape does not chang any more, and still remains asymmetric, in contrast to the spectra of nonmagnetic Lu. This shows that the collapse of the splitting is not complete.

To be more quantitative, the least-squares-fit analysis used before for Lu was applied to all spectra, but with *two* symmetric Lorentzians of equal intensity for S_2. The width of the two components was allowed to vary in order to account for possible spin-dependent lifetime effects. The average lifetime of the two components was held constant for all temperatures. In this way a consistent description of the five series of spectra in Fig. 6 was obtained as given by the solid lines through the data points. For all systems, the energy splitting $\Delta E(T)$ decreases upon heating, reaching a finite residual value in the paramagnetic phase, as summarized in Fig. 7. Due to the thermal broadening and the small magnitude of the splitting, the two components are not well resolved around T^* any more. Therefore, their energy positions cannot be determined with high accuracy and the splitting determined from the fit analysis depends to some extent on the widths of the lines. These uncertainties, however, have been included in the error bars of Fig. 7, determined by varying these parameters to the limits, where reasonable fits could be obtained. Data were taken at least up to room temperature, which is far above the various T^* of Tb, Dy, and Ho. For the case of Gd, the temperature range is limited by the onset of oxygen desorption at 350 K. In none

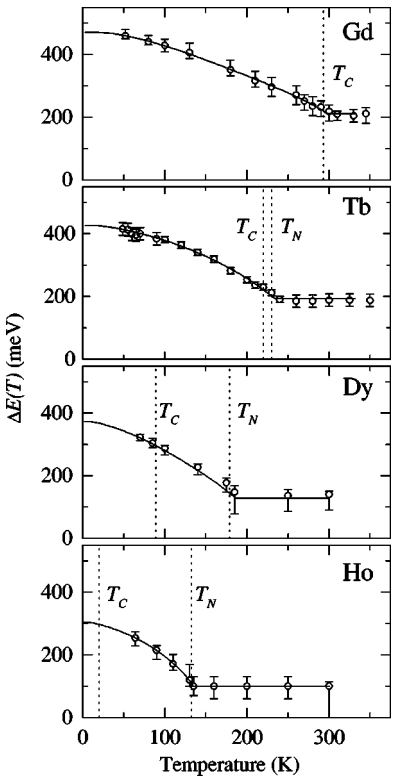

FIG. 7. Temperature dependence of the energy splittings $\Delta E(T)$ of the oxygen-induced surface states (solid circles) as determined from the least-squares-fit analyses of the spectra in Fig. 5. The solid lines through the data points represent the result of a model fit as described in the text.

of the systems has any change of the spectral shape, which might indicate a further decrease of the splitting at higher temperatures, been observed above T^*.

In order to obtain a reliable extrapolation of the splitting to zero Kelvin, an analysis of the temperature dependence was performed. According to Nolting *et al.*, the temperature dependence of the magnetic splitting in a local-moment system can be described by the sum of two contributions.[11] The first part considers the influence of the long-range magnetic order and is proportional to the $4f$ magnetization. The second part takes the spin-exchange processes between $4f$ and valence electrons into account and contains a more complicated functional of the electron self-energies for both valence-electron-spin directions. The latter is responsible for the constant residual splitting above T^* and hence was assumed to be essentially temperature independent. The temperature-dependent part of the magnetic splittings of S_2 was described by a mean-field model, successfully applied before to the case of a monolayer of Eu on Gd.[44] This model uses the coupling within the surface layer, J_{ss}, and the coupling between surface layer and bulk, J_{sb}, both relative to the bulk value, J_{bb}, as adjustable parameters. The magnetization of each layer is calculated by taking into account the influence of all nearest-neighbor moments weighted by the respective coupling strengths. This leads to a set of coupled equations that can be solved self-consistently.[44]

The fits using this model are shown in Fig. 7 as solid lines

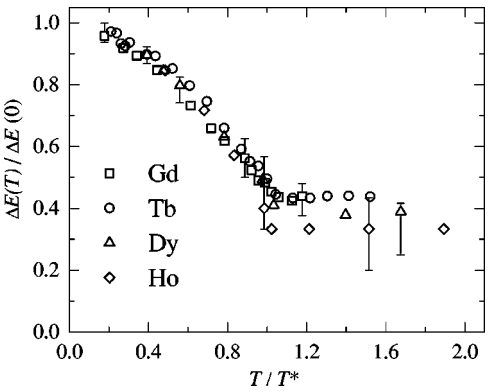

FIG. 8. Temperature-dependent splittings $\Delta E(T)$ of the oxygen-induced states S_2 of Gd, Tb, Dy, and Ho, normalized to the respective zero-temperature splitting $\Delta E(0)$. T^* denotes the respective highest magnetic ordering temperature.

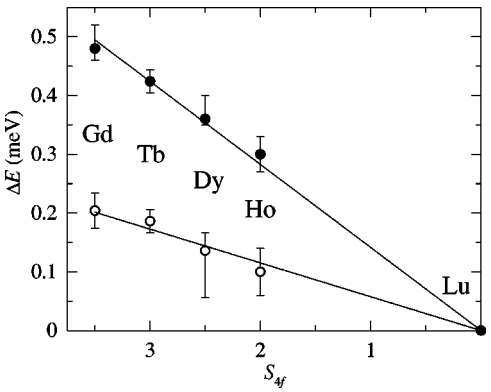

FIG. 9. Zero-Kelvin splitting (filled circles) and high-temperature residual splitting (open circles) of S_2 plotted versus the $4f$-spin moment S_{4f}.

through the data points. The good agreement between the model calculations and the data for both ferromagnetic and antiferromagnetic lanthanides indicates that the temperature-dependent part of the magnetic splitting is essentially determined by the magnetic order within the surface layer. Since the coupling parameters depend sensitively on the curvatures of the $\Delta E(T)$ curves, they cannot be derived with sufficient accuracy from the present set of data, even for Gd and Tb with comparably large splittings and high T^*. Nevertheless, a consistent picture is obtained in all cases, with weaker coupling within the surface-oxide layer than in the bulk, as expected for an oxide system with a reduced density of conduction states at E_F.

Even though a precise determination of the coupling parameters from the energy splittings of Fig. 7 is not possible, the analysis allows to extract the zero-Kelvin splittings $\Delta E(0)$ of Gd to Ho with reasonably high accuracy. The resulting normalized splittings $\Delta E(T)/\Delta E(0)$ are plotted in Fig. 8 as a function of the reduced temperature, T/T^*. The figure demonstrates the systematic behavior of the magnetic splitting of S_2 across the lanthanide series, independent of the type of magnetic order. Such a behavior has been observed before for the Δ_2 bulk band, indicating that these states are sensitive to the magnetization of the ferromagnetically ordered close-packed planes rather than the total magnetization.[19] This applies even more to the oxygen-induced states of the present study, which are strongly localized within the topmost layer and are therefore not influenced by the long-range magnetic order along the c axis.

The magnitude of the splittings, both $\Delta E(0)$ and the persisting splitting above T^*, is plotted versus the $4f$-spin moment in Fig. 9. As in the case of the Δ_2 bulk states,[19] the proportionality to S_{4f} is clearly observed for both components, with the residual splitting amounting to about 40% of $\Delta E(0)$. This proportionality is expected,[45] if the exchange integral does not strongly change across the lanthanide series. In fact, within the error bars of the present experiment, the effective exchange-coupling constant J_{eff} is found to be constant and can be obtained from the slopes in Fig. 9 according to $\Delta E = 2J_{eff}\mu_B S_{4f}$,[45] where μ_B denotes the Bohr magneton.

The effective coupling constants are given in Table. I, together with the numbers for the Δ_2 bulk states[19] and the surface state of the clean surfaces, obtained from STS data.[18] The strongest coupling is observed for the bulk Δ_2 states in the vicinity of Γ, with a magnitude that is not too far from that calculated for $5d$ conduction electrons in the vicinity of E_F.[45] In the latter calculation, a slight increase of J_{eff} across the lanthanide series due to lanthanide contraction is obtained, while for the valence states of the present investigation, no indication for such behavior is found. Interestingly, the numbers are smaller in the case of the more localized surface states, both for the clean and oxygen-covered lanthanide surfaces. From the increased localized character compared to the Δ_2 states, one might anticipate, on the contrary, a stronger local interaction with the $4f$ electrons. An analogous result, however, was found at the close-packed surface of Ce metal, namely, a weaker hybridization between the $4f$ and $5d$ states in the presence of the localized surface state as compared to the bulk.[46] The smaller splitting of the oxygen-induced surface state is not surprising, taking into account the considerable mixing with the O-$2p$ states, which

TABLE I. Effective exchange-coupling constants J_{eff} between various valence states and the $4f$ states.

State	$J_{eff}\mu_B$ (meV)
Δ_2 at Γ[a]	134±8
Surface state $[\Delta E(0)]$[b]	100
Oxygen-induced surface state $[\Delta E(0)]$[c]	70±6
Oxygen-induced surface state (residual splitting)[c]	28±6
$5d$ states at E_F[d]	88 (Gd) to 106 (Ho)

[a]Reference 19.
[b]STS data from Ref. 18.
[c]This work.
[d]Calculated, from Ref. 45.

will reduce the overlap with the $4f$ wave function at the lanthanide site.

IV. SUMMARY

The temperature-dependent valence-electronic structure of local-moment magnetic systems is currently the subject of extended studies, both theoretically and experimentally. In this context, a surface-oxide phase on the close-packed surfaces of the heavy lanthanide metals was discussed here, providing interesting possibilities for a quantitative study of the influence of magnetic ordering on the valence-electronic structure. This system can be readily prepared by oxygen adsorption and is stable for more than one day under ultrahigh-vacuum conditions. The oxide layer exhibits metallic character and magnetic order in a temperature range determined by the respective ordering temperature of the underlying metal. A particularly interesting feature of the system is a surface state that is fully occupied and hence can be readily studied by angle-resolved photoemission. This oxygen-induced surface state closely resembles that of the clean (0001) surfaces, situated in the same gap of the projected bulk band structure. However, it is characterized by a significant admixture of O-$2p$ states and is closer to the lower edge of the band gap. The magnetic splitting of the oxygen-induced surface states is proportional to the $4f$-spin moment and displays features of spin-mixing behavior as expected for more localized valence states in a local-moment magnetic system: While the splitting decreases substantially with increasing temperature, a constant finite value persists above the highest magnetic ordering temperature. For Gd and Tb, this finite splitting can be directly seen in the spectra; for Dy and Ho it results from a consistent data analysis. The temperature dependence of the splittings can be readily described in terms of a mean-field model for a magnetic monolayer coupled to a magnetic substrate, taking an additional temperature-independent contribution into account. It was shown here that this behavior is independent of the type of magnetic order, as it is systematic across the heavy lanthanide series, with no anomalous behavior for antiferromagnetic systems. While these conclusions are based on the systematic behavior of the energy splitting only, the oxygen-induced surface state provides a tool to study the temperature-dependent spin-mixing behavior in local-moment magnetic systems quantitatively by spin-resolved photoemission.

ACKNOWLEDGMENTS

The authors thank P. Jensen and W. Nolting for valuable discussions. This work was supported by the German ministry for science and technology, BMBF, Project No. SF8 KEC8, the Deutsche Forschungsgemeinschaft, Project Nos. Sfb-290/TPA06 and Ka-564/2, as well as the European Community (EFRE). C.M. acknowledges support from the Alexander von Humboldt Foundation.

[1] J. Jensen and A.R. Macintosh, *Rare Earth Magnetism* (Clarendon Press, Oxford, 1991).
[2] M.A. Ruderman and C. Kittel, Phys. Rev. **96**, 99 (1954); T. Kasuya, Prog. Theor. Phys. **16**, 45 (1956); K. Yosida, Phys. Rev. **106**, 893 (1957).
[3] S.K. Sinha, in *Handbook on the Physics and Chemistry of Rare Earths*, edited by K.A. Gschneidner, Jr. and LeRoy Eyring (North-Holland, Amsterdam, 1978), Vol. 1, p. 489.
[4] W. C. Koehler, in *Magnetic Properties of Rare Earth Metals*, edited by R. J. Elliott (Plenum, London, 1972), Vol. 10, p. 81.
[5] D. Gibbs, D.E. Moncton, K.L. D'Amico, J. Bohr, and B.H. Grier, Phys. Rev. Lett. **55**, 234 (1985).
[6] G. Helgesen, J.P. Hill, T.R. Thurston, and D. Gibbs, Phys. Rev. B **52**, 9446 (1995).
[7] S.B. Dugdale, H.M. Fretwell, M.A. Alam, G. Kontrym-Sznajd, R.N. West, and S. Badrzadeh, Phys. Rev. Lett. **79**, 941 (1997).
[8] H.M. Fretwell, S.B. Dugdale, M.A. Alam, D.C.R. Hedley, A. Rodriguez-Gonzalez, and S.B. Palmer, Phys. Rev. Lett. **82**, 3867 (1999).
[9] B. Kim, A.B. Andrews, J.L. Erskine, K.J. Kim, and B.N. Harmon, Phys. Rev. Lett. **68**, 1931 (1992).
[10] L.M. Sandratskii and J. Kübler, Europhys. Lett. **23**, 661 (1993).
[11] W. Nolting, T. Dambeck, and G. Borstel, Z. Phys. B: Condens. Matter **94**, 409 (1994).
[12] A.V. Fedorov, K. Starke, and G. Kaindl, Phys. Rev. B **50**, 2739 (1994).
[13] D. Li, J. Pearson, S.D. Bader, D.N. McIlroy, C. Waldfried, and P.A. Dowben, Phys. Rev. B **51**, 13 895 (1995).
[14] E. Weschke, C. Schüßler-Langeheine, R. Meier, A.V. Fedorov, K. Starke, F. Hübinger, and G. Kaindl, Phys. Rev. Lett. **77**, 3415 (1996).
[15] M. Donath, B. Gubanka, and F. Passek, Phys. Rev. Lett. **77**, 5138 (1996).
[16] M. Bode, M. Getzlaff, S. Heinze, R. Pascal, and R. Wiesendanger, Appl. Phys. A: Mater. Sci. Process. **66**, S121 (1998).
[17] M. Getzlaff, M. Bode, S. Heinze, R. Pascal, and R. Wiesendanger, J. Magn. Magn. Mater. **184**, 155 (1998).
[18] M. Bode, M. Getzlaff, A. Kubetzka, R. Pascal, O. Pietzsch, and R. Wiesendanger, Phys. Rev. Lett. **83**, 3017 (1999).
[19] C. Schüßler-Langeheine, E. Weschke, Chandan Mazumdar, R. Meier, A.Yu. Grigoriev, G. Kaindl, C. Sutter, D. Abernathy, G. Grübel, and Manuel Richter, Phys. Rev. Lett. **84**, 5624 (2000).
[20] E.C. Stoner, Proc. R. Soc. London, Ser. A **165**, 372 (1938); J.C. Slater, Phys. Rev. **49**, 537 (1936); **49**, 931 (1936).
[21] L. M. Sandratskii and J. Kübler, in *Magnetism and Electronic Correlations in Local-Moment Systems: Rare-Earth Elements and Compounds*, edited by M. Donath, W. Nolting, and P.A. Dowben (World Scientific, Singapore, 1998), p. 271.
[22] J. Krizek and K.N.R. Taylor, J. Phys. F: Met. Phys. **5**, 774 (1975).
[23] Yu.V. Knyazev and M.M. Noskov, Phys. Status Solidi B **80**, 11 (1977).
[24] A.B. Beznosov, V.V. Eremenko, and V.P. Gnezdilov, J. Magn. Magn. Mater. **43**, 243 (1984).
[25] Yu.V. Knyazev and L.M. Sandratskii, J. Phys.: Condens. Matter **3**, 9667 (1991).

[26] R. Wu, C. Li, A.J. Freeman, and C.L. Fu, Phys. Rev. B **44**, 9400 (1991).
[27] D. Li, J. Zhang, P.A. Dowben, and M. Onellion, Phys. Rev. B **45**, 7272 (1992).
[28] G. Kaindl, A. Höhr, E. Weschke, S. Vandré, C. Schüßler-Langeheine, and C. Laubschat, Phys. Rev. B **51**, 7920 (1995).
[29] E. Weschke and G. Kaindl, J. Electron Spectrosc. Relat. Phenom. **75**, 233 (1995).
[30] R. Meier, E. Weschke, A. Bievetski, C. Schüßler-Langeheine, Z. Hu, and G. Kaindl, Chem. Phys. Lett. **292**, 507 (1998).
[31] C. Schüßler-Langeheine, R. Meier, H. Ott, Z. Hu, Chandan Mazumdar, A.Y. Grigoriev, G. Kaindl, and E. Weschke, Phys. Rev. B **60**, 3449 (1999).
[32] E. Weschke, C. Schüßler-Langeheine, R. Meier, G. Kaindl, C. Sutter, D. Abernathy, and G. Grübel, Phys. Rev. Lett. **79**, 3954 (1997).
[33] D. Weller and D.D. Sarma, Surf. Sci. **171**, L425 (1986).
[34] E. Navas, K. Starke, C. Laubschat, E. Weschke, and G. Kaindl, Phys. Rev. B **48**, 14 753 (1993).
[35] S.D. Kevan and W. Eberhardt, in *Angle-Resolved Photoemission*, edited by S.D. Kevan (Elsevier, Amsterdam, 1992), p. 99.
[36] C. Puglia, A. Nilsson, B. Hernnäs, O. Karis, P. Bennich, and N. Mårtensson, Surf. Sci. **342**, 119 (1995).
[37] R.A. DiDio, D.M. Zehner, and E.W. Plummer, J. Vac. Sci. Technol. A **2**, 852 (1984).
[38] J. Zhang, P.A. Dowben, D. Li, and M. Onellion, Surf. Sci. **329**, 177 (1995).
[39] F. Hulliger and T. Siegrist, Z. Phys. B **35**, 81 (1979).
[40] B. Johansson and N. Mårtensson, in *Handbook on the Physics and Chemistry of Rare Earths*, edited by K.A. Gschneidner, Jr. and S. Hüfner (North-Holland, Amsterdam, 1987), Vol. 10, p. 361.
[41] N. Mårtensson, B. Reihl, and R.D. Parks, Solid State Commun. **41**, 573 (1982).
[42] M. Bodenbach, A. Höhr, C. Laubschat, G. Kaindl, and M. Methfessel, Phys. Rev. B **50**, 14 446 (1994).
[43] G.A. Mulhollan, K. Garrison, and J.L. Erskine, Phys. Rev. Lett. **69**, 3240 (1992).
[44] E. Arenholz, K. Starke, G. Kaindl, and P.J. Jensen, Phys. Rev. Lett. **80**, 2221 (1998).
[45] R. Ahuja, S. Auluck, B. Johansson, and M.S.S. Brooks, Phys. Rev. B **50**, 5147 (1994).
[46] E. Weschke, A. Höhr, G. Kaindl, S.L. Molodtsov, S. Danzenbächer, M. Richter, and C. Laubschat, Phys. Rev. B **58**, 3682 (1998).